To Heart via Liver: a Study on Prognostic Stratification of Heart Disease in MASLD Patients using Machine Learning Models

Pierangela Bruno[1,**], Antonio Cirella[2,**], Ernesto Di Cesare[3], Gianluigi Greco[1], Antonella Guzzo[4], Pierpaolo Palumbo[3], Silvano Junior Santini[2], Gaia Sinatti[2], Pierpaolo Vittorini[2], Francesco Calimeri[1] and Clara Balsano[2]

[1]*Department of Mathematics and Computer Science, University of Calabria, Rende, Italy*
[2]*Department of Clinical Medicine, Life, Health & Environmental Sciences-MESVA, University of L'Aquila, Italy*
[3]*Department of applied clinical sciences and biotechnology, university of L'Aquila, Italy*
[4]*Department of Informatics, Modeling, Electronics, and Systems Engineering-University of Calabria, Rende, Italy*

Abstract

Accurate cardiovascular (CV) risk assessment is relevant for asymptomatic individuals, in particular for those at risk for cardiovascular diseases (CVD). Metabolic-associated fatty liver disease (MASLD), previously known as non-alcoholic fatty liver disease (NAFLD), is recognized as a critical independent risk factor for increased CV morbidity and mortality. With a prevalence of 25% in the general population, MASLD is the leading cause of chronic liver diseases and is strongly associated with the development of coronary artery disease (CAD). Coronary CT is widely used to detect CAD, and it can also assess liver steatosis, providing valuable prognostic information for at-risk patients.

In this paper, we present a study on methods for performing prognostic stratification of CAD risk in asymptomatic MASLD patients using machine learning (ML) approaches. In particular, we conducted a retrospective analysis of clinical data from 60 patients who underwent Coronary CT at L'Aquila Hospital (Italy) between 2017 and 2021. Dataset includes significant features, such as radiodensity (Hounsfield Unit), calcium score (Agatston score), and liver fibrosis (Fib-4 score and APRI).

We compared several ML algorithms (Logistic Regression, Support Vector Classifier (SVC), Random Forest, Extreme Gradient Boosting, K-Nearest Neighbors (KNN), Naive Bayes), with the main goal of performing binary classification tasks and creating a model able to differentiate between healthy patients and those affected by both MASLD and CVD. SVCs emerged as the best-performing models, achieving an AUC of 94%, an accuracy of 95%, and a recall of 94%. Our approach offers a robust and accurate tool for predicting CAD risk in MASLD patients, providing a valuable contribution to clinical practice for early CV risk stratification and management.

Keywords

Machine Learning, Coronary Artery Disease, Metabolic-associated fatty liver disease,

1. Introduction

Nonalcoholic fatty liver disease (NAFLD) recently emerged as one of the most widespread liver conditions globally, affecting nearly a quarter of the world's population; its incidence is expected to grow progressively in the future. NAFLD is characterized by fat accumulation in the liver and encompasses a wide range of liver conditions, from simple fat deposition (steatosis) to more severe forms such as hepatitis, fibrosis, cirrhosis, and hepatocellular carcinoma [1, 2]. Due to the strong association with obesity and metabolic syndrome, NAFLD was recently redefined as metabolic-associated fatty liver disease (MASLD), to better reflect its metabolic origin [3].

3rd AIxIA Workshop on Artificial Intelligence For Healthcare (HC@AIxIA 2024)
*P.Bruno is corresponding author
**First authors contributed equally to this paper.
pierangela.bruno@unical.it (P. Bruno); cirella.nt@gmail.com (A. Cirella); ernesto.dicesare@univaq.it (E. Di Cesare); gianluigi.greco@unical.it (G. Greco); antonella.guzzo@unical.it (A. Guzzo); pierpaolo.palumbo@univaq.it (P. Palumbo); silvanojunior.santini@univaq.it (S. J. Santini); gaia.sinatti@graduate.univaq.it (G. Sinatti); pierpaolo.vittorini@univaq.it (P. Vittorini); francesco.calimeri@unical.it (F. Calimeri); clara.balsano@univaq.it (C. Balsano)

Currently, cardiovascular disease (CVD) is reported as the primary cause of death and illness in MASLD patients. It is estimated that nearly half of the adult population in the United States has some degree of liver fat, adding significantly to the national healthcare and economic burden [4, 5, 6]. Because of the overlap in risk factors such as obesity, insulin resistance, high blood pressure, and abnormal cholesterol levels, MASLD has been proposed as an independent risk factor for CVD [7, 8]. Hence, conducting a precise cardiovascular risk assessment in asymptomatic MASLD patients is crucial for preventing and properly managing related complications.

Coronary CT, an imaging technique that does not require contrast agents, is an effective mean for detecting CVD through the measurement of coronary artery calcification (CAC), which is in turn a reliable indicator of future cardiac events in both symptomatic and asymptomatic individuals [9]. Recent researches have demonstrated that non-contrast CT can also detect liver fat, thereby extending its clinical utility [10, 11]; this enables the possible to evaluate both CAC and hepatic steatosis during a single Coronary CT scan, offering a more comprehensive assessment of cardiovascular risk [12].

To evaluate liver fibrosis, we used two non-invasive markers: the AST-to-platelet ratio index (APRI) and the Fibrosis-4 (FIB-4) score, which are calculated using clinical parameters like AST, ALT, platelet count, and age. These methods provide a safer and reliable alternative to liver biopsy for determining fibrosis severity [13, 14].

In this study, we explored the use of machine learning (ML) techniques to analyze clinical data and create predictive models aimed at evaluating cardiovascular risk in individuals with MASLD. Our main goal is to improve the accuracy of risk stratification, thereby offering a valuable tool for early intervention and enhancing clinical outcomes in this at-risk population. The main contributions of this work are summarized next.

- We construct a new dataset that includes demographic information (such as gender, age, and comorbidities), blood test results (including ALT, AST, BUN, creatinine, hemoglobin, platelets, and white blood cells), as well as derived metrics like FIB-4 and APRI. Additionally, radiological data such as liver density, liver-to-spleen ratio, and Coronary Artery Calcium (CAC) score are incorporated.
- We conduct a comprehensive comparison of various ML algorithms, including Logistic Regression, Support Vector Classifier (SVC), Random Forest, Extreme Gradient Boosting (XGBoost), K-Nearest Neighbors (KNN), and Naive Bayes. These algorithms were employed in a binary classification task to differentiate between healthy individuals and those suffering from both MASLD and CVD.
- We perform several experiments to identify the most suitable algorithms; also, we optimized the models through hyperparameter tuning to fulfil the best possible performance. Specifically, the effectiveness of these models was assessed using several metrics, including accuracy, precision, recall, and the area under the curve (AUC).
- We employed SHapley Additive exPlanations (SHAP) to interpret the results of the best-performing model, providing insights into feature importance, enhancing the explainability and the understanding classification model.

The remainder of the paper is structured as follows. In Section 2 we provide a detailed description of our approach; then, we illustrate a careful and thorough experimental activity aimed at assessing it in Section 3. Results are analyzed and discussed in Section 4, and our conclusions are eventually drawn in Section 5.

2. Proposed approach

With this study, we aimed to develop and identify an optimal binary classifier of CAD in asymptomatic MASLD patients. We conducted a comparative analysis to evaluate the performance of widely used supervised ML classification algorithms [15]: Logistic Regression, SVC, Random Forest, XGBoost, KNN, and Naive Bayes. We briefly describe the algorithms next, and report the workflow of the herein reported approach in Figure 1.

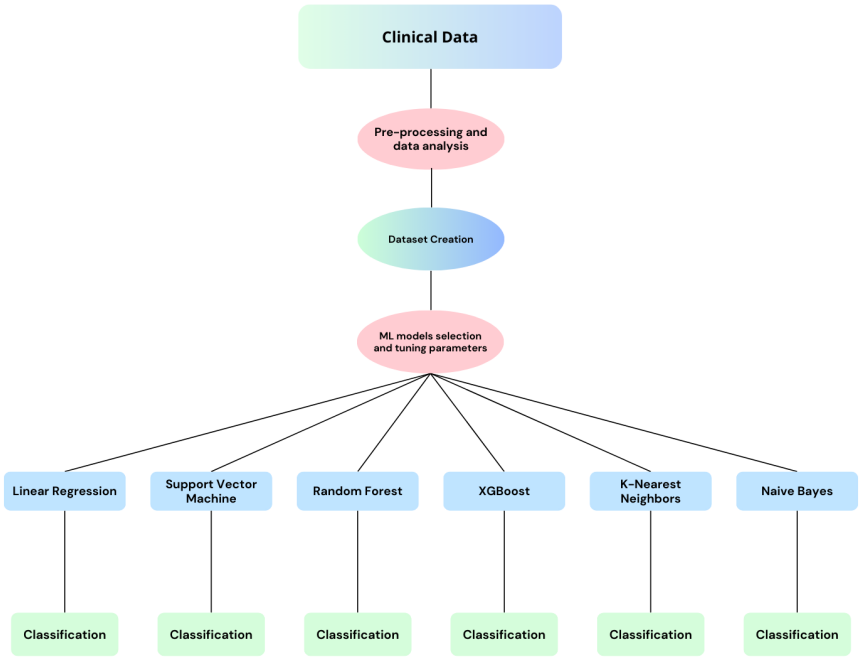

Figure 1: Example of workflow of our approach.

1. Logistic Regression [16] models the relationship between a dependent variable and one or more independent variables using a logistic function, providing the probability of a binary outcome.
2. SVC [17] is a supervised learning algorithm that constructs hyperplanes in a high-dimensional space to separate different classes of data points. It is effective for high-dimensional datasets and can be extended to non-linear classification through the use of kernel functions. SVC is known for its robustness to overfitting, especially in cases where the number of dimensions exceeds the number of samples.
3. Random Forest [18] is an ensemble method that constructs multiple decision trees during training and outputs the mode of the classes for classification tasks. It improves accuracy and robustness by reducing overfitting and provides insights into feature importance.
4. XGBoost [19] is a powerful gradient boosting algorithm that builds an ensemble of trees sequentially, where each new tree corrects errors made by the previous ones. It offers high predictive accuracy, efficient handling of large datasets, and robustness against overfitting and missing data.
5. KNN [20] is a non-parametric classification algorithm that assigns a class to a data point based on the classes of its nearest neighbours in the feature space. The number of neighbours k is a hyperparameter that can be tuned. KNN is simple to implement and works well for small datasets but can be computationally intensive for large datasets.
6. Naive Bayes [21] is a family of probabilistic algorithms based on applying Bayes' theorem with strong (naive) independence assumptions between the features. Despite its simplicity, Naive Bayes can be very effective for text classification and other tasks, particularly when the dimensionality of the input is high.

3. Experimental Analysis

In the following section, we will detail the dataset acquisition and partitioning process, the model training procedures, and the hyperparameter tuning strategies that were critical to optimizing ML models.

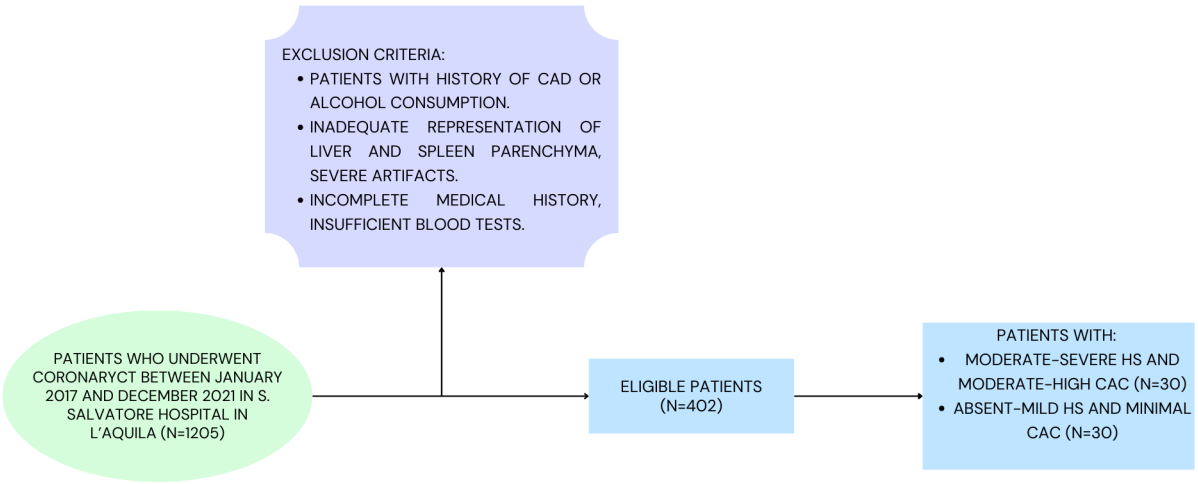

Figure 2: Patients acquisition and exclusion criteria.

3.1. Dataset Acquisition and Description

As for data, 1205 patients were selected who underwent Coronary CT between 2017 and 2021 at San Salvatore Hospital in L'Aquila (Italy); patients were excluded based on incomplete liver or spleen scans, severe artifacts, alcohol abuse or insufficient medical history and blood tests. Figure 2 summarizes the data collection and exclusion criteria. All patient information was anonymized prior to measurement. A retrospective analysis was conducted on clinical, laboratory, and imaging data from 402 subjects (217 males, 185 females). The CT images were acquired using a prospective cardiosynchronized technique and pre-contrast scans were evaluated for Coronary Artery Calcium (CAC) score (Agatston score) [22] and liver density (measured in Hounsfield units, HU). The images were acquired using a Toshiba Aquilion scanner with the following settings: 320-slice CT (100 kV, 46 mAs, 0.35s, 0.5mm slice thickness, and 280mm scan range). Regarding the presence of CAC, patients were classified into four risk categories based on the Agatston score: 0–10, 11–100, 101–400, and over 400 [23]. Two senior radiology residents, with over 5 years of experience each, selected the appropriate Coronary CT exams containing complete liver and spleen parenchyma on non-contrast CT sequences first; then, they independently identified the liver images for ROI placement, blinded to the patient's clinical history. To assess reproducibility, each resident repeated the ROI measurements on their colleague's selected images, and the mean attenuation values were compared with the initial measurements. The Fib-4 and APRI scores were calculated as a non-invasive marker of hepatic fibrosis from common parameter like blood tests. Specifically, we evaluated several Fib-4 cut-off thresholds commonly used in clinical practice. The first cut-off is the most widely adopted, indicating absence of fibrosis for values below 1.3 and presence of fibrosis for values above 2.67 (Fib-4 I). The second threshold categorizes fibrosis for values below 2 and above 2.67(Fib-4 II), while the third uses <1.45 to indicate no fibrosis and >3.25 (Fib-4 III) to indicate significant fibrosis [24, 25].

On unenhanced CT, normal liver attenuation is approximately 64 HU, about 10 HU higher than the spleen and the fat's attenuation leads to a proportional decrease in liver density. To measure liver and spleen density in nonenhanced Coronary CT sequences, the correct axial slice must be identified. Given that hepatic lipid concentration is uniformly distributed, precise placement of Regions of Interest (ROIs) is crucial, avoiding large vessels and confounding factors like artifacts. Each ROI was standardized to an area of 2.00 ± 0.15 cm^2. Three ROIs were placed in the liver following a modified Couinaud's method: one in the left lobe (segment II or III) and two in the right lobe (segments VII/VIII and V/VI), positioned at least 5–10 mm from the liver periphery. The final liver density was calculated as the arithmetic mean of these three ROIs. Additionally, two ROIs were placed in the anterior and posterior regions of the spleen, and the average value was used for analysis [26]. Liver steatosis was determined using liver attenuation or the liver-to-spleen (L/S) ratio. In unenhanced CT, moderate steatosis corresponds to

Table 1
Dataset distribution between training and testing according to male, female, and class of interest (Healthy/Unhealthy).

Type of Dataset	N. Patients	Male	Female	Healthy	Unhealthy
Train	42	23	19	21	21
Test	18	7	11	9	9

Table 2
Tuning Parameters, Selected Values, and Best Values for Machine Learning Algorithms.

Algorithm	Tuning Parameter	Selected Values	Best Value
Logistic Regression	Regularization (C)	0.001, 0.01, 0.1, 1, 10, 100	1
	Max Iterations (max_iter)	100, 500, 1000	1000
	Penalty	l1, l2	l2
SVC	Kernel	Linear, Polynomial, Radial Basis (RBF)	Radial Basis (RBF)
	Regularization (C)	0.001, 0.01, 0.1, 1, 10, 100	1
Random Forest	Number of Trees (n_estimators)	10, 50, 100, 200	100
	Maximum Depth (max_depth)	None, 10, 20, 30	20
	Minimum Samples per Split (min_samples_split)	2, 5, 10	2
XGBoost	Learning Rate (eta)	0.01, 0.1, 0.3	0.1
	Number of Trees (n_estimators)	50, 100, 200, 500	100
	Maximum Depth (max_depth)	3, 6, 9	3
KNN	Number of Neighbours (n_neighbours)	3, 5, 7, 9	5
Naive Bayes	Distribution Type	Gaussian, Multinomial	Gaussian
	Smoothing Parameter (alpha)	$1e^{-09}$,$1e^{-02}$ 0.1, 0.5, 1	$1e^{-09}$

approximately 40 HU, while a steatotic liver was defined as having a hepatic-to-spleen attenuation ratio of less than 1.0 on unenhanced CT. The sensitivity and specificity of CT for detecting mild liver steatosis are 57% and 88% respectively; while for higher-grade steatosis CT sensitivity increases to 72% and specificity to 95% [27, 28, 29].

We classified the cohort into five groups:

- moderate to high CAC (>101 Agatston) and moderate to severe HS (<40 HU),
- minimal CAC (<10 Agatston) and absent HS (>60 HU),
- moderate to high CAC (>101 Agatston) and absent HS (>60 HU),
- minimal CAC (<10 Agatston) and moderate-severe HS (<40 HU),
- with minor CAC (10–100 Agatston) and minor HS (40–60 HU).

In our experiments, we selected patients belonging to two classes: healthy and patients that suffer from both CAC and HS. Then, we selected 60 patients and we split into training and testing set, as described in Table 1.

3.2. Experimental setting

For training our models, we split the dataset into training (70%) and testing (30%) sets. For the training phase, we performed Grid Search to find the optimal hyperparameters for each model. Details are provided below; The key hyperparameters tuned for each model are detailed in Table 2.

- *Logistic Regression.* The regularization strength (denoted by parameter C) was set to 1, striking a balance between preventing overfitting and maintaining model accuracy. The maximum number of iterations (*max_iter*) has been increased and set to 1000 in order to ensure proper convergence, especially in more complex cases. Additionally, the l2 penalty was selected, given that it is commonly preferred for regularization for avoiding large coefficient magnitudes.
- *SVC.* We chose the Radial Basis Function (RBF) kernel, due to its ability to handle non-linear data. The regularization parameter C was set to 1, providing a good trade-off between margin maximization and misclassification tolerance. This combination allowed the SVC to generalize effectively, while managing complexity.

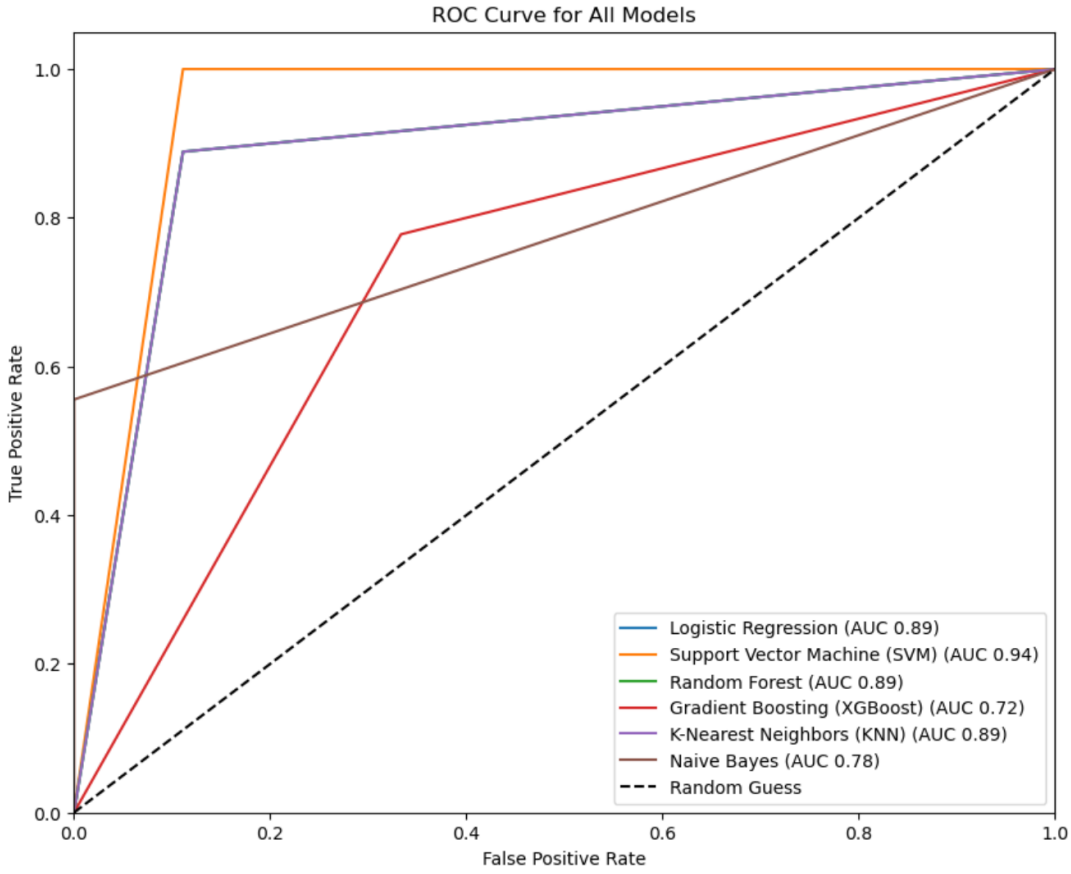

Figure 3: ROC curve results for each ML algorithm.

- *Random Forest*. The number of trees (*n_estimators*) has been set to 100, as this configuration showed to improve accuracy without introducing excessive computational overhead. A maximum depth of 20 was selected for the trees, so to prevent overfitting while maintaining model performance.
- *XGBoost*. The learning rate has been set to 0.1, thus allowing the model to make gradual updates during training and avoid overshooting the optimal solution. The maximum depth of the trees has been set to 3, providing a good balance between model complexity and generalization.
- *KNN*. We found that setting the number of neighbours (*n_neighbours*) to 5 yielded the most reliable results.
- *Naive Bayes*. The Gaussian distribution has been selected because of its suitability for continuous data. The smoothing parameter (alpha) was set to $1e^{-09}$, which helped to improve model stability.

These parameter configurations were carefully selected based on performance metrics such as accuracy, precision, recall, and AUC, ensuring that each algorithm was optimized for the task at hand.

4. Results and Discussion

A detailed analysis of the dataset revealed a significant positive correlation between liver attenuation and the Agatston score (P<0.01) and a significant association between Fib-4 and Agatston (P<0.01).

To assess the viability of our approach, we tested the ML algorithm for binary classification using clinical data from 60 patients.

Results are shown in Table 3. Furthermore, we compute the Receiver Operating Characteristic (ROC) curve, a key tool for evaluating the performance of classification models. It illustrates the trade-off between sensitivity and specificity across various thresholds, with the area under the curve (AUC) serving as a measure of the model's ability to differentiate between classes. A higher AUC indicates

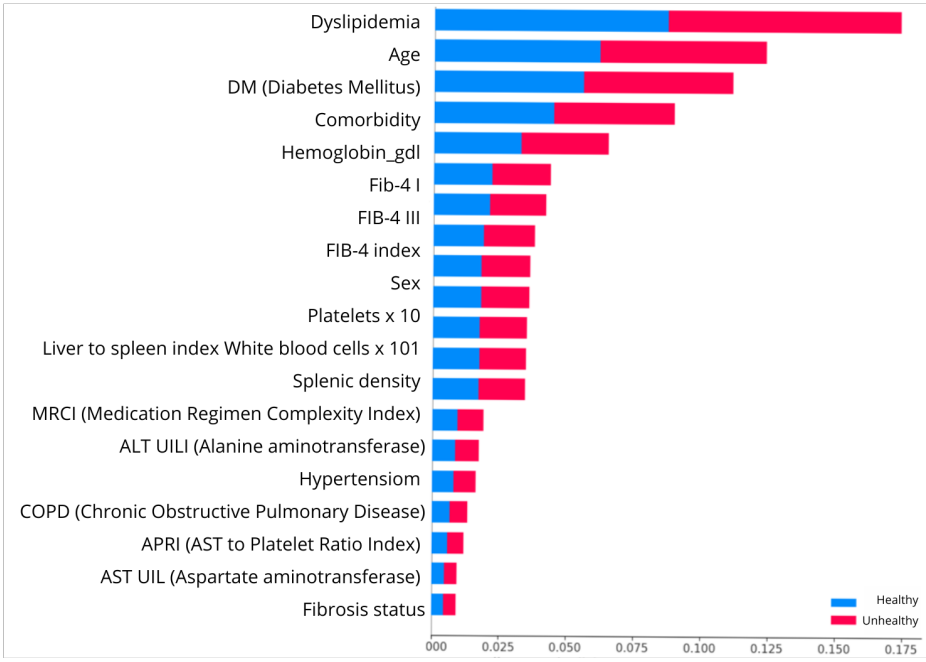

Figure 4: Feature importance of each feature in the SVC model.

Table 3
Performance Metrics for Different Machine Learning Algorithms.

Algorithm	Accuracy	Precision	Recall	Specificity	Sensitivity	AUC
Logistic Regression	0.89	0.89	0.89	0.89	0.89	0.89
SVC	**0.94**	**0.95**	**0.94**	0.89	**0.99**	**0.94**
Random Forest	0.89	0.89	0.89	0.89	0.89	0.89
XGBoost	0.72	0.73	0.72	0.67	0.78	0.72
KNN	0.89	0.89	0.89	0.89	0.89	0.89
Naive Bayes	0.78	0.85	0.78	**0.99**	0.56	0.78
Mean Values	0.85	0.86	0.85	0.87	0.83	0.85

better model performance. Figure 3 presents the ROC curve results obtained from the ML algorithms. A proper ROC curve analysis reveals that SVC and Random Forest appear to be the most effective models for identifying cardiovascular risk in MASLD patients, as indicated by their high AUC values and good positioning of their ROC curves.

In particular, SVC stands out among evaluated models showing the highest performance, achieving strong accuracy, precision, and an impressive sensitivity of 99%; hence, it appears to be an ideal tool for medical applications where identifying every positive case is crucial. This model's ability to balance precision and recall highlights its robustness, particularly in complex decision boundaries. In comparison, Random Forest and KNN also performed well, offering balanced metrics across all categories; however, their performance was slightly behind SVC, especially in sensitivity, where SVC outperformed them. Interestingly, Logistic Regression, despite being a simpler model, demonstrated valuable results, closely matching Random Forest and KNN.

It is worth noting that XGBoost, which usually excels in different domains, underperformed on our problem achieving the lowest accuracy, precision, and recall scores. This could be due to the relatively small nature of the dataset, which might have precluded XGBoost from leveraging its strengths in large or high-dimensional data. Naive Bayes, on the other hand, had high precision and specificity, but its poor sensitivity (56%) suggests it failed to capture many true positives, making it a risky choice for healthcare tasks where missing positive cases could have severe consequences.

Overall, we can conclude that SVC is the best choice in the pool, given its superior metrics, particularly

in critical areas like sensitivity. Random Forest and KNN results as reliable alternatives, while Naive Bayes and XGBoost may not be suitable for this specific kind of datasets.

4.1. Explainability

The interpretability of ML models has become increasingly important, especially in healthcare applications where decisions can significantly impact patient outcomes [30]. In this context, in order to provide some insights into the contribution of each feature to model's predictions, we make use of SHAP. This method helps bridge the gap between complex model behavior and human understanding, making it easier for clinicians to trust and utilize these tools in practice.

In our study, we focus on the results of SVC, which in our experiments emerged as the top-performing algorithm. By applying SHAP, we gained a detailed understanding of how various clinical features influence the SVC's predictions for both classes. The summary plot in Figure 4 shows the feature importance of each feature in the SVC model.

The SHAP results for class 1 (unhealthy) revealed that the most influential features contributing to the classification included Dyslipidemia, with an importance score of 0.086749, indicating that lipid abnormalities are a significant risk factor for this group. Variables Age at 0.061625 and Diabetes Mellitus (DM) with 0.056511 immediately follow, underscoring the role of these demographic and metabolic factors in cardiovascular risk assessment. Similar results are obtained for class 0. It is worth noting that features such as Dyslipidemia and Diabetes Mellitus (DM) showed similar SHAP values for both healthy and MASLD patients with CVD; this clearly indicates that these factors are significant risk indicators across both populations, reinforcing their importance in clinical assessments and decision-making; notably, this aligns with the current background medical knowledge, as confirmed by physicians.

5. Conclusion

This study demonstrated the potential of machine learning (ML) techniques in analyzing clinical data and creating predictive models for evaluating cardiovascular risk in individuals with MASLD. Among the evaluated models, SVC emerged as the most effective, achieving high accuracy and sensitivity, making it particularly valuable for early diagnosis in asymptomatic patients.

The application of this model in clinical settings could significantly enhance risk stratification, enabling the timely identification and management of high-risk patients. Building on this foundation, we plan to conduct additional experiments in future work, such as implementing k-fold cross-validation and investigating alternative performance metrics, like the Matthews Correlation Coefficient (MCC), which may provide further insights into our classification tasks.

We also intend to expand our dataset to include more samples and incorporate multimodal data, such as geometric features extracted from CT images, to enhance the predictive power of the models.

Acknowledgments

This work has been partially supported by PON "Ricerca e Innovazione" 2014-2020, CUP: H25F21001230004. Francesco Calimeri is member of the Gruppo Nazionale Calcolo Scientifico - Istituto Nazionale di Alta Matematica (GNCS-INdAM).

Statements

The study was approved by the Internal Review Board of L'Aquila, with all participants providing informed consent.

References

[1] G. Vernon, A. Baranova, Z. Younossi, Systematic review: the epidemiology and natural history of non-alcoholic fatty liver disease and non-alcoholic steatohepatitis in adults, Alimentary pharmacology & therapeutics 34 (2011) 274–285.

[2] C. Estes, H. Razavi, R. Loomba, Z. Younossi, A. J. Sanyal, Modeling the epidemic of nonalcoholic fatty liver disease demonstrates an exponential increase in burden of disease, Hepatology 67 (2018) 123–133.

[3] M. Eslam, P. N. Newsome, S. K. Sarin, et al., A new definition for metabolic dysfunction-associated fatty liver disease: an international expert consensus statement, Journal of Hepatology 73 (2020) 202–209.

[4] G. Bedogni, V. Nobili, C. Tiribelli, Epidemiology of fatty liver: an update, World journal of gastroenterology: WJG 20 (2014) 9050.

[5] Q. M. Anstee, A. Mantovani, H. Tilg, G. Targher, Risk of cardiomyopathy and cardiac arrhythmias in patients with nonalcoholic fatty liver disease, Nature Reviews Gastroenterology & Hepatology 15 (2018) 425–439.

[6] E. T. Oni, A. S. Agatston, M. J. Blaha, J. Fialkow, R. Cury, A. Sposito, R. Erbel, R. Blankstein, T. Feldman, M. H. Al-Mallah, et al., A systematic review: burden and severity of subclinical cardiovascular disease among those with nonalcoholic fatty liver; should we care?, Atherosclerosis 230 (2013) 258–267.

[7] A. Mellemkjær, M. B. Kjær, D. Haldrup, H. Grønbæk, K. L. Thomsen, Management of cardiovascular risk in patients with metabolic dysfunction-associated steatotic liver disease (2020).

[8] J. H. Moon, S. Jeong, H. Jang, B. K. Koo, W. Kim, Metabolic dysfunction-associated steatotic liver disease increases the risk of incident cardiovascular disease: a nationwide cohort study, EClinicalMedicine 65 (2023).

[9] H. Isma'eel, D. Min, L. Al-Shaar, R. Hachamovitch, S. Halliburton, J. Gentry, B. Griffin, P. Schoenhagen, D. Phelan, Assessing level of agreement for atherosclerotic cardiovascular disease risk categorization between coronary artery calcium score and the american college of cardiology/american heart association cardiovascular prevention guidelines and the potential impact on treatment recommendations, The American journal of cardiology 118 (2016) 1480–1485.

[10] J. Starekova, D. Hernando, P. J. Pickhardt, S. B. Reeder, Quantification of liver fat content with CT and MRI: state of the art, volume 301, Radiological Society of North America, 2021.

[11] E. Chartampilas, Imaging of nonalcoholic fatty liver disease and its clinical utility, Hormones 17 (2018) 69–81.

[12] C. J. Boyce, P. J. Pickhardt, D. H. Kim, A. J. Taylor, T. C. Winter, R. J. Bruce, M. J. Lindstrom, J. L. Hinshaw, Hepatic steatosis (fatty liver disease) in asymptomatic adults identified by unenhanced low-dose ct, American Journal of Roentgenology 194 (2010) 623–628.

[13] A. G. Shah, A. Lydecker, K. Murray, B. N. Tetri, M. J. Contos, A. J. Sanyal, N. C. R. Network, et al., Comparison of noninvasive markers of fibrosis in patients with nonalcoholic fatty liver disease, Clinical gastroenterology and hepatology 7 (2009) 1104–1112.

[14] J.-L. Jin, H.-W. Zhang, Y.-X. Cao, H.-H. Liu, Q. Hua, Y.-F. Li, Y. Zhang, Y.-L. Guo, N.-Q. Wu, C.-G. Zhu, et al., Liver fibrosis scores and coronary atherosclerosis: novel findings in patients with stable coronary artery disease, Hepatology International 15 (2021) 413–423.

[15] J.-J. Beunza, E. Puertas, E. García-Ovejero, G. Villalba, E. Condes, G. Koleva, C. Hurtado, M. F. Landecho, Comparison of machine learning algorithms for clinical event prediction (risk of coronary heart disease), Journal of biomedical informatics 97 (2019) 103257.

[16] P. Schober, T. R. Vetter, Logistic regression in medical research, Anesthesia & Analgesia 132 (2021) 365–366.

[17] S. Vijayakumar, S. Wu, Sequential support vector classifiers and regression., in: IIA/SOCO, 1999.

[18] Y. Qi, Random forest for bioinformatics, Ensemble machine learning: Methods and applications (2012) 307–323.

[19] T. Chen, Xgboost: extreme gradient boosting, R package version 0.4-2 1 (2015).

[20] L. E. Peterson, K-nearest neighbor, Scholarpedia 4 (2009) 1883.
[21] G. I. Webb, E. Keogh, R. Miikkulainen, Naïve bayes., Encyclopedia of machine learning 15 (2010) 713–714.
[22] O. Dzaye, R. Dudum, M. Mirbolouk, O. A. Orimoloye, A. D. Osei, Z. A. Dardari, D. S. Berman, M. D. Miedema, L. Shaw, A. Rozanski, M. Holdhoff, K. Nasir, J. A. Rumberger, M. J. Budoff, M. H. Al-Mallah, R. Blankstein, M. J. Blaha, Validation of the coronary artery calcium data and reporting system (cac-drs): Dual importance of cac score and cac distribution from the coronary artery calcium (cac) consortium, Journal of Cardiovascular Computed Tomography 14 (2020) 12–17. URL: https://www.sciencedirect.com/science/article/pii/S1934592519300620. doi:https://doi.org/10.1016/j.jcct.2019.03.011.
[23] I. Isgum, M. Prokop, M. Niemeijer, M. A. Viergever, B. Van Ginneken, Automatic coronary calcium scoring in low-dose chest computed tomography, IEEE transactions on medical imaging 31 (2012) 2322–2334.
[24] S. McPherson, T. Hardy, J.-F. Dufour, S. Petta, M. Romero-Gomez, M. Allison, C. P. Oliveira, S. Francque, L. Van Gaal, J. M. Schattenberg, et al., Age as a confounding factor for the accurate non-invasive diagnosis of advanced nafld fibrosis, Official journal of the American College of Gastroenterology| ACG 112 (2017) 740–751.
[25] Y. Sumida, M. Yoneda, H. Hyogo, Y. Itoh, M. Ono, H. Fujii, Y. Eguchi, Y. Suzuki, N. Aoki, K. Kanemasa, et al., Validation of the fib4 index in a japanese nonalcoholic fatty liver disease population, BMC gastroenterology 12 (2012) 1–9.
[26] E. K. Speliotes, J. M. Massaro, U. Hoffmann, M. C. Foster, D. V. Sahani, J. N. Hirschhorn, C. J. O'Donnell, C. S. Fox, Liver fat is reproducibly measured using computed tomography in the framingham heart study, Journal of gastroenterology and hepatology 23 (2008) 894–899.
[27] J. J. Xu, M. R. Boesen, S. L. Hansen, P. S. Ulriksen, S. Holm, L. Lönn, K. L. Hansen, Assessment of liver fat: Dual-energy ct versus conventional ct with and without contrast, Diagnostics 12 (2022) 708.
[28] Y. Kodama, C. S. Ng, T. T. Wu, G. D. Ayers, S. A. Curley, E. K. Abdalla, J. N. Vauthey, C. Charnsangavej, Comparison of ct methods for determining the fat content of the liver, American Journal of Roentgenology 188 (2007) 1307–1312.
[29] N. Poyraz, H. Özer, İ. Baloğlu, C. Kadıyoran, P. D. Yılmaz, A. L. Sertdemir, K. Türkmen, Liver–spleen ratio: Can it be used for the prediction of coronary artery disease?, Anatolian Journal of Cardiology 26 (2022) 762.
[30] A. Vellido, The importance of interpretability and visualization in machine learning for applications in medicine and health care, Neural computing and applications 32 (2020) 18069–18083.